LA-UR-98- -3536

Los Alamos National Laboratory is operated by the University of California for the United States Department of Energy under contract W-7405-ENG-36

CONF-980803--

TITLE: PLANE IMPACT RESPONSE OF PBX 9501 BELOW 2 GPA

AUTHOR: Jerry J. Dick, A. Richard Martinez and Robert S. Hixson
LANL, Los Alamos, NM 87545

SUBMITTED TO: Eleventh Symposium (International)
on Detonation, August 31 - September 4, 1998

Los Alamos
Los Alamos National Laboratory
Los Alamos, New Mexico 87545

DISCLAIMER

Portions of this document may be illegible in electronic image products. Images are produced from the best available original document.

PLANE IMPACT RESPONSE OF PBX 9501 BELOW 2 GPA. *

J. J. Dick,† A. R. Martinez, and R. S. Hixson
Los Alamos National Laboratory, Los Alamos, New Mexico 87545

The plane impact response of PBX 9501 was measured below 2 GPa using a light-gas gun facility. Time-resolved wave profiles were obtained in a state of uniaxial strain for impact stresses between 0.3 to 1.2 GPa. The dynamic strength of PBX 9501 was measured at high strain rates in both compression and tension. The Hugoniot equation of state was measured.

INTRODUCTION

The problem of accidental detonation of explosive due to a mechanical insult is of continuing concern. The insult may not begin as a shock, but data from plane impact experiments provide equation of state data and the mechanical response at high strain rates in a well-defined state of uniaxial strain. In these experiments we have measured impact response from 200 MPa to 2 GPa and impact velocities down to 120 m/s. There was essentially no existing data in this region for PBX 9501. The low end overlaps the range of stresses found in the spigot test, Steven test [1], and other multidimensional tests. [2] The results should enhance understanding of impact tests on PBX's and serve as a basis for testing models used in computation of hazards problems.

EXPERIMENTAL TECHNIQUE

Plane impact experiments were performed using a light-gas gun facility. Time-resolved wave profiles of particle velocity were measured using magnetic gauges in one of two configurations or using VISAR[1] laser interferometry. The experimental arrangements are depicted in Figs. 1 to 3. In the case of magnetic gauges, in-material wave profiles were measured; in the case of VISAR experiments the profiles were measured at the interface between the material and a PMMA (polymethylmethacrylate) window. The laser beam is reflected from the mirror at the interface with spot size of about 0.6 mm at the center of the sample. The average target chamber temperature was 20.7 ± 2.3°C.

The PBX 9501 impactors for symmetric impact experiments with PBX 9501 were 50.8 mm in diameter. The VISAR experiment 1054 at 1.2 GPa, had a z-cut quartz impactor 50.8 mm in diameter flush-mounted in an aluminum projectile, but backed by PMMA 8 mm thick. The remaining experiments had impactors 57.2 mm in diameter and were backed by a microballoon or

*Work performed under the auspices of the U. S. Department of Energy and partially supported by the Department of Defense/Office of Munitions under the Joint DoD/DOE Munitions Technology Program and the Explosives Technology Program at LANL.

†Electronic mail: jjd @lanl.gov

[1]VISAR stands for velocity interferometer system for any reflector.

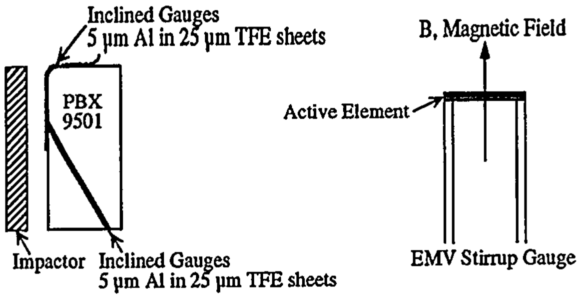

FIGURE 1. Schema of the gun impact experiment with MMV instrumentation. Gauge positions are marked in red. The gauge leads and insulation are marked in blue.

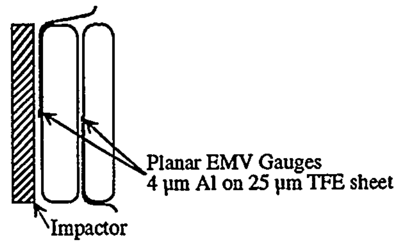

FIGURE 2. Schema of the gun impact experiment with stirrup gauge instrumentation. Gauge positions are marked in red. The gauge leads and insulation are marked in blue.

polyurethane foam with a density of about 0.48 g/cm^3.

The samples of PBX 9501 were 50.8 mm in diameter. With one exception, all PBX 9501 samples were from 13.5 x 13.5 x 3.5-inch blocks hydrostatically from Holston lot 89C730-010. The average density of the samples was 1.827 $\pm$ 0.001 g/cm^3. For VISAR experiments the samples were placed in a 51 mm dia hole in the aluminum target plate 6 mm thick. The impact face of the sample was nearly flush with the front face of the plate. For magnetic experiments the samples were mounted on the front of the plate so that the gauges were about 15 to 25 mm above the plate. In this way the dynamic measurements were made before the shock wave reached the metal plate and disturbed the magnetic field.

Magnetic Gauging Experiments

Magnetic gauges operate according to Maxwell's third relation. The shock-induced motion of the gauge active element is perpendicular to the magnetic field. Therefore, the induced voltage is $\epsilon = Bul$, where B is the magnetic field of about 0.750 kgauss, u is the particle velocity induced by the shock in mm/μs, and l is the length of the gauge active element in cm. The length is 0.6 to 1.0 cm.

Two types of magnetic gauging experiments were performed on PBX 9501. Magnetic impulse and particle velocity (MIV) gauge packages consisting of 5 nested gauges of each type are placed side by side sandwiched between sheets of Teflon 25 μm thick (See Fig. 1.). The nested particle velocity gauges are 6 to 10 mm wide. The active elements were made of aluminum 5 μm thick. The gauge active elements are spaced 2 mm apart in the sandwich so that when placed in the sample at an angle of 30° the gauges are successively 1 mm deeper into the explosive sample. Some experiments were performed with two sets of nested particle velocity (MMV, multiple magnetic velocity) gauges.

The second type consists of two particle velocity gauges (EMV, electromagnetic velocity, stirrup) with 10-mm-wide active elements. These gauges are emplaced parallel to the shock impact face as in Fig. 2. One is placed on the impact face, and one is placed between two pieces of explosive of varying thicknesses. The gauge package consists of the aluminum gauge on one sheet of Teflon.

VISAR Experiments

For VISAR studies, PMMA (Mil. Spec. P-5425D, preshrunk) windows were used, Fig. 3. The mirrors were either vapor-plated aluminum or 13 μm thick aluminum foil. The samples of PBX 9501 were 50.8 mm in diameter. Two to four piezoelectric pins were emplaced on the impact face of the sample on opposite sides of a diameter. The time difference between shock arrival at these pins and the shock arrival signal recorded by the VISAR allowed measurement of transit time through the crystal and from that the wave velocities. It is important to account for the difference in signal travel times to the digitizing oscilloscopes for the two types of signals.

The measurement system used was a push-pull, VISAR system. [3] The light was transported from the argon-ion laser to the target and thence to the interferometer table with fiber optics. The fiber optic probe on the target was obtained from

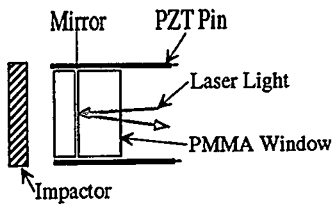

FIGURE 3. Schema of the gun impact experiment with VISAR instrumentation.

Valyn International. The overall response time of the system is about 3 ns at the shock-wave arrival time.

SUMMARY OF EXPERIMENTAL RESULTS

Wave profiles of particle velocity vs time were obtained for PBX 9501 at about 0.3, 0.6, 1.2, 1.6, and 2.0 GPa. For PBX 9501 there were no reliable Hugoniot data below 2 GPa. Hugoniot equation of state data were obtained on PBX 9501 and HMX single crystals. No Hugoniot data for HMX single crystals below 35 GPa.

In PBX 9501 multiple embedded magnetic gauge records were obtained at 0.3, 0.6 and 1.2 GPa with 5 particle velocity histories at 1.4 to 5.4 mm. These were symmetric impact experiments with PBX 9501 impactors. In this way the final particle velocity is required to be half the accurately measured projectile velocity. This is a check on the accuracy of the MIV gauges. At 0.3 GPa 2 experiments with stirrup gauges at 5.4 mm depth were performed in order to check repeatability and agreement with the multiple embedded gauges that are in the sample on a plane slanted 30° with respect to the shock plane. Similarly, one stirrup gauge experiment was performed at 0.6 GPa. At 0.3 and 0.6 GPa stirrup gauge experiments were performed with 8-mm thick PBX 9501 samples and VISAR experiments with 10 mm thick samples. In addition, wave profiles were obtained with VISAR instrumentation on samples 5 mm thick at 1.2, 1.6, 1.8 and 2.0 GPa. There was evidence of initiation at 1.6 to 2.0 GPa. [4]

HUGONIOT OF PBX 9501

Hugoniot data for PBX 9501 are displayed in Fig. 4. A fit to the Hugoniot data obtained here and some of the data in Ref. [5] for densities 1.832 to 1.844 g/cm^3 is

$$U_S = 2.40 + 2.39u_p, \quad 0 < u < 0.9 \text{ mm}/\mu s, \quad (1)$$

where U_S is shock velocity or wave velocity at half the maximum particle velocity, and u_p is final particle velocity. The standard errors of the fit parameters are 0.03, and 0.07, respectively. The root mean squared (RMS) error of the shock velocity is 0.09 mm/μs. The average Hugoniot elastic limit point is U_S=2.84 mm/μs and u_p=0.025 mm/μs. The Hugoniot data are tabulated in Ref. [4].

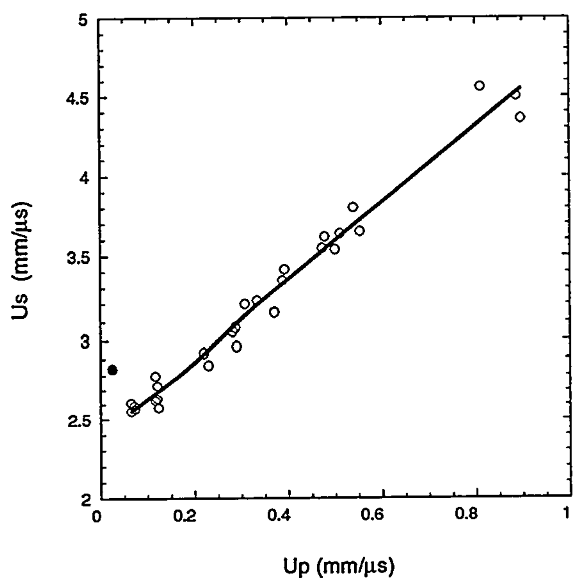

FIGURE 4. PBX 9501 shock velocity vs particle Hugoniot data. The solid blue circle is the average Hugoniot elastic limit point.

The Hugoniot curve is the locus of end states on the thermodynamic equilibrium surface for the material for shocks taking the material from the initial state to the final state. The Hugoniot jump conditions for conservation of mass and momentum apply only to discontinuities or steady waves. For the unsteady waves up to 600 MPa, approximate Hugoniot states were obtained by taking the transit time for the particle velocity on the wave front equal to half the final particle velocity for the entire wave.

Volumetric strain is $-(V-V_0)/V_0 = 1-V/V_0$, where V_0 is the specific volume in the initial state. The Hugoniot data represent the locus of end states for the compressive waves. The locus describes a curve on the thermodynamic surface of the material. Ten percent uniaxial strain or compression is reached at about 1.8 GPa and 20% at about 7 GPa. CHECK THE NUMBERS

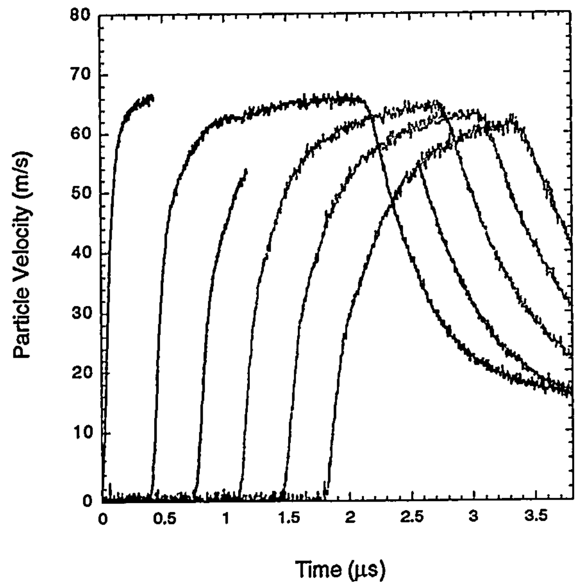

FIGURE 5. In-material MMV gauge records in PBX 9501 at 303 MPa in a symmetric impact experiment, 1116. Gauge positions are 1.32 to 5.27 mm in from impact face. Half the impact velocity is 66.2 m/s. The middle part of the second record at 2.32 mm was lost.

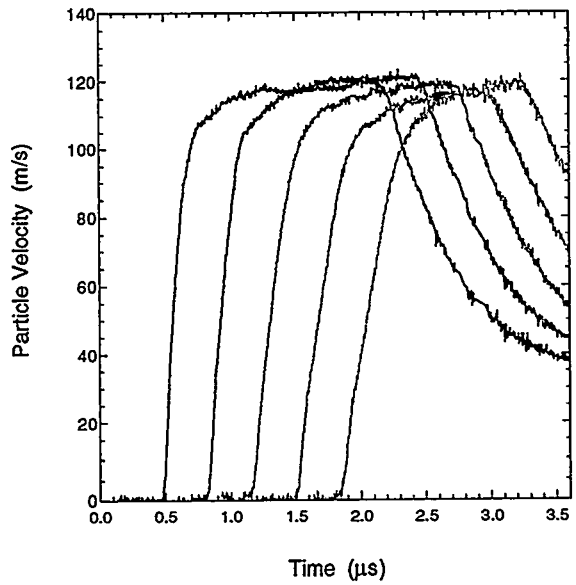

FIGURE 6. In-material MIV gauge records in PBX 9501 at 560 MPa in a symmetric impact experiment, 1049. Gauge positions are 1.38 to 5.32 mm in from impact face. Half the impact velocity is 116 m/s.

The moduli of PBX 9501 are rate dependent. From sound speeds [6] the Young's modulus for PBX 9501 is 9.56 GPa. In contrast, a value of 1.01 ± 0.18 GPa was measured in Instron tests. [7] The ratio of high to low strain rate Young's modulus is 9.5.

The longitudinal modulus, $\rho_0 C_L^2$, of PBX 9501 is 16.8 GPa. For the two HMX crystal orientations the average value is 26.6 ± 0.3 GPa. In comparison, the c_{11} elastic constant of HMX is about 20 GPa and the c_{33} is 21 GPa. [8]

WAVE PROFILE MEASUREMENTS IN PBX 9501

Wave profiles were measured in PBX 9501 at about 0.3, 0.6, 1.2, 1.6, 1.8, and 2 GPa. Embedded, 30°, nested magnetic experiments were performed at 0.3, 0.6, and 1.2 GPa. The experiments at 0.3 GPa had a stirrup gauge emplaced on the center of the impact face. The measured profiles for the Holston lot 89C730-010 are shown in Fig. 5 to 6.

At 0.31 GPa we see long rise times that evolve with propagation distance and a subtle two-wave structure developing at the last two gauges (Fig. 5). There is a change in slope just below 30 m/s. The first wave is the elastic wave, and the change in slope defines the elastic limit. The inelastic wave is dispersive and unsteady. The unloading wave is recorded as well. The same behavior is noted at 0.6 GPa (Fig. 6). At 1.2 GPa the wave has sharpened up considerably, but there is an apparent shoulder at the end of the sharp rise (Fig. ??). At late times the agreement with half the projectile velocity is quite good at 1.2 GPa, within 1% for the last 4 gauges. At 0.6 GPa the particle velocity at late times is 0.4 to 3.0% high. At 0.3 GPa the final state on the first embedded gauge is 0.6% low in experiment 1116. At subsequent gauges the final state is not reached before the rarefaction arrives.

Wave Profile Measurements in PBX 9501 near 310 MPa

In addition to the MMV gauging measurements, three stirrup gauge measurements were made (two at 5.4 mm and one at 8 mm) as well as a VISAR measurement with a 10 mm thick sample. The two stirrup gauges at 5.4 mm and at 307 and 345 MPa agree very well with the MMV record at 5.27 mm from experiment 1116 at 303 MPa. This shows that the profile measurements are repeatable on PBX 9501 at the same density, from the same lot, and pressed in the same way.

This also demonstrates that gauges emplaced at 30° to the impact plane agree well with gauges emplaced parallel to the impact plane and the wave front.

The VISAR experiment measures the particle velocity history at the interface between the explosive and the PMMA mirror. In addition, the experiments did not have exactly the same impact stress. In order to display all profiles on the same plot, it was decided to normalize the measured particle velocities by the expected final particle velocities. For symmetric impact the final particle velocity is half the projectile velocity; for VISAR and experiments with two stirrup gauges it was the value calculated from the known Hugoniots including the Hugoniot of PBX 9501 using Joe Fritz's MACRAME characteristics code.

A summary of experiments near 310 MPa for the same lot of PBX 9501 is displayed in Fig. 7. A front-surface impact record is shown from experiment 1072. The interferometric record for the VISAR experiment at 10 mm was only half a fringe for the fringe constant used. This short of a record resulted in poor accuracy for the particle velocity profile obtained. The final level was about 10% low. Therefore the record was scaled by 1.10 in order to bring it in line with the other records and the final particle velocity calculated by MACRAME.

Wave Profile Measurements in PBX 9501 near 580 MPa

The results of experiment 1049 at 560 MPa are displayed in Fig. 6. The rise times are sharper than at 310 MPa but the wave is still unsteady, the profile changing as it propagates. A stirrup gauge experiment 1117 was performed at about 5.37 mm for comparison with the last gauge in experiment 1049 that had the gauges emplaced at 30° to the impact plane at 5.39 mm. The agreement in wave front profiles is good, similar to the results at 310 MPa. Both types of gauge emplacements perform well. The slanted gauges appear to show a sharper change in slope between the elastic and inelastic waves at a relative particle velocity of about 0.25. A summary of all records near 580 MPa plotted as relative particle velocity is shown in Fig. 8.

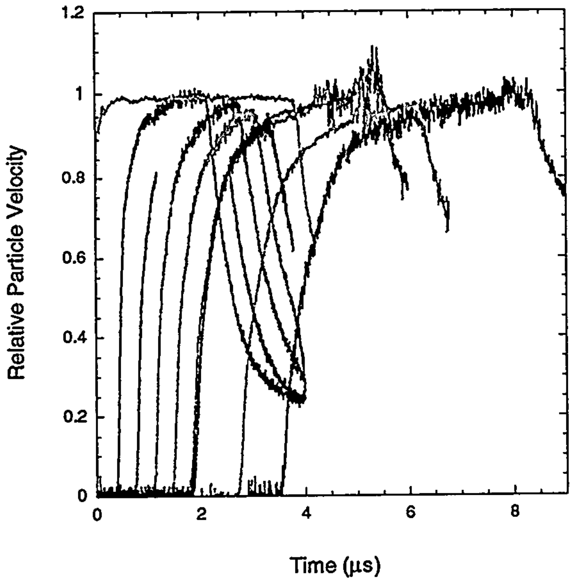

FIGURE 7. Experimental wave profiles in PBX 9501 near 310 MPa for lot 89C730-010 hydrostatically pressed to a density of 1.827 ± 0.001 g/cm^3. The two orange profiles are from stirrup gauges for experiment 1072. The last record is from a VISAR experiment 1061.

Wave Profile Measurements in PBX 9501 at 1.2 GPa

The comparison of the nested, embedded, magnetic gauge records from experiment 1058 at depths from 1.37 to 5.33 mm are compared to the VISAR record for experiment 1054 at 1.20 GPa with a sample 5.04 mm thick in Fig. 9. The rise times agree quite well, and the VISAR record confirms the hesitation in the wave front rise at 92 to 95% of the final state.

The z-cut quartz impactor in the VISAR experiment was only 2.55 mm thick. The shock velocity in the impactor was 6.46 mm/μs; therefore the rarefaction overtook the wave front before the final state was reached after 5 mm of wave propagation in PBX 9501.

Elastic Wave Strength in PBX 9501

The elastic wave is discernible in experiments near 300 and 600 MPa. In some measurements the end of the elastic wave is delineated by a subtle two-wave structure, in others by a change in slope of the wave profile. Corresponding yield stresses in uniaxial stress Y are calculated from [9]

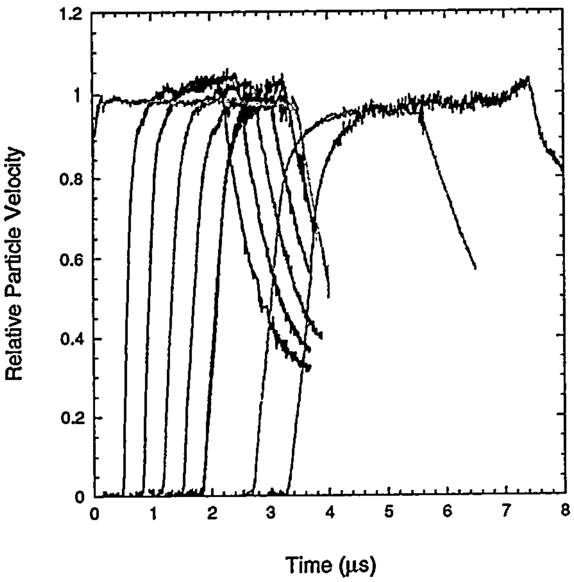

FIGURE 8. Experimental wave profiles in PBX 9501 at 560 to 600 MPa. The two orange profiles are for experiment 1073. The last record is from a VISAR experiment 1060.

$$Y = \left[\frac{1-2\nu}{1-\nu}\right]\sigma_x^{HEL}, \qquad (2)$$

where ν is Poisson's ratio and σ_x^{HEL} is the Hugoniot elastic limit. The value of ν for PBX 9501 is 0.36 from sound speed measurements. [6] For samples from lot 89C730-010 the average Hugoniot elastic limit is 123 ± 8 MPa for impact stresses of about 310 MPa and 150 ± 15 MPa for impact stresses of about 580 MPa. The corresponding yield stresses are 54 and 66 MPa. The results for experiment 1042 at 600 MPa using material that was ram-pressed from another lot has the largest Hugoniot elastic limit 219 MPa and a yield stress of 96 MPa. It had a density of 1.835 g/cm^3.

For comparison, a Hugoniot elastic limit of 140 MPa was measured in Composition B. [6,10] A very different, ramp-like precursor was observed for PBX 9502. [11] The longitudinal stress value at the end of the ramp was 73 MPa. Chhabildas and Kipp measured the maximum shear stress in PBX 9404 using pressure-shear impact loading. [12] Their result was 40 MPa. The yield stress is twice that, 80 MPa. From Vickers hardness tests a value of 66 MPa was given for the flow stress for HMX by Mohan, Bhasu, and Field [13] giving a value of 132 MPa for Y.

It is interesting to note that the threshold velocity for explosion in the spigot test or the Steven test corresponds to about 100 MPa in PBX 9501 in the center after impact, close to the Hugoniot elastic limit. The threshold velocity may be correlated to the threshold for inelastic, irreversible, dissipative deformation.

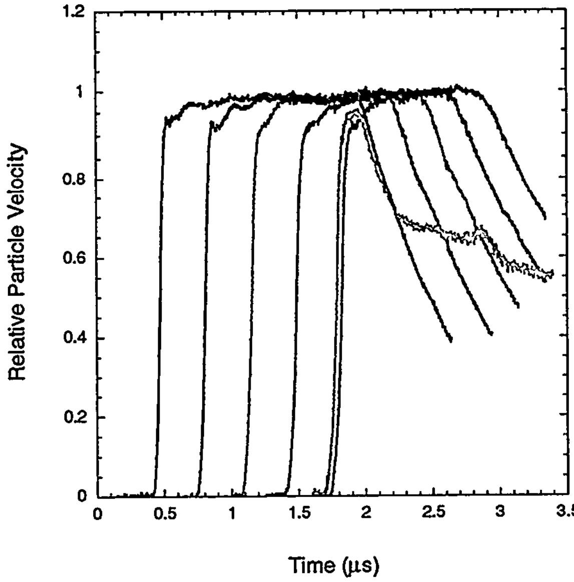

FIGURE 9. Experimental wave profiles in PBX 9501 at 1.2 GPa. The nested magnetic gauges are at 1.37 to 5.33 mm depth. The VISAR record is at 5.04 mm.

PBX 9501 Strength vs Strain Rate

Using Instron and Hopkinson bar instrumentation Los Alamos National Laboratory workers have measured the ultimate compressive strength on the same lot of PBX 9501 pressed to the same density by the same technique. [7,14,4] The ultimate compressive strength is the maximum compressive stress achieved. Yield stresses are proportional to and less than the ultimate compressive strengths. [7,14]

Earlier measurements of PBX 9501 ultimate compressive strength are listed in Ref. [5] for several temperatures. There is strong temperature dependence of strength. The strain rate is not specified but may have been 0.00083 s^{-1}. The density is 1.844 g/cm^3. At 24°C the ultimate compressive strength is given as 7.86 MPa. This value is slightly lower than values for the current material. [7] In other earlier work on another lot of PBX 9501 reported in Dobratz's compendium, [15] the ultimate compressive strength in Instron tests is about 6 MPa at a strain rate of 10^{-5} s^{-1}, 33 MPa at 750 s^{-1}, and 43 MPa at 10^3 s^{-1}. For comparison, the yield stresses calculated form Hugoniot elastic limits in the current work raged from 54 to 96 MPa. There is significant strain-rate dependence of the yield stress. The state of strain may also be important. Mechanical failure in PBX 9501 and other PBXs at low strain rates has been studied in detail by others. [7,16]

PBX 9501 Rise Times and Strain Rates

The rise times of the profiles in the experiments in PBX 9501 were measured. The rise time was taken as the rise time from 10% to 90% of the total signal rise. Since the approach to final state is so gradual at low stresses, it is difficult to pick off the precise time at times closer to the final state than 90%. The values are displayed in Fig. 10. One notes that at 0.3 and 0.6 GPa impact stresses, the rise times increase with propagation distance out to about 8 mm. It appears that the waves become steady after 7 to 8 mm of propagation distance at these impact stresses. At 1.2 GPa the rise time increases from 60 to about 100 ns between 2 and 4 mm.

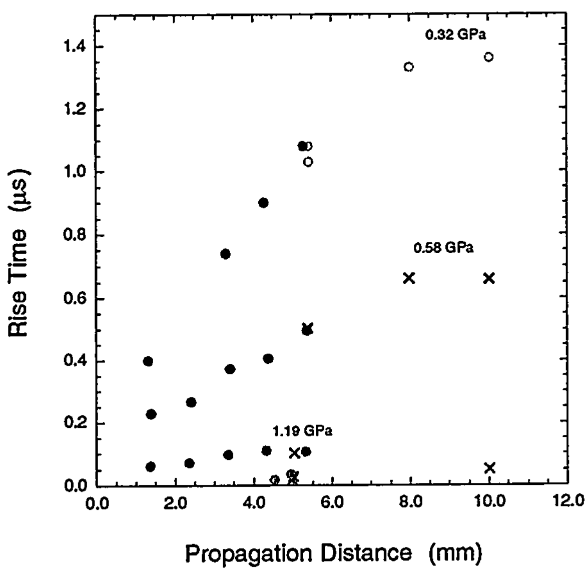

FIGURE 10. Compressive wave rise time vs wave propagation distance for several impact stress levels in PBX 9501. The black exes are near 1.6 GPa, the orange circle near 1.8 GPa, and the green circle near 2 GPa.

It is worth noting that the plastic wave in HMX single crystals 3 mm thick impacted at 1.4 GPa has a rise time of about 122 ns. In pentaerythritol tetranitrate (PETN) crystals unsteady plastic waves were observed. [17] Therefore, some of the dispersed, unsteady wave behavior seen in PBX 9501 may be inherent in the HMX.

The behavior of decreasing rise time with increasing impact stress has been noted before as the typical response to shocks. Swegle and Grady noted that for metals and oxides that the peak strain rate in the shock was consistent with a power-law relation between the peak strain rate and the shock stress; [18] the peak strain rate for the total strain varies as the fourth power of the shock stress. They obtained the peak strain rate in the shock profile by numerically differentiating the measured profile.

For comparing the PBX 9501 data to this relation, the strain rate in the wave front was taken as the total strain divided by the 10 to 90% rise time at sample thicknesses where the wave had become steady. The comparison is shown in Fig. 11. The line is described by 0.0395 times the strain rate to the one-fourth power. The data for PBX 9501 agree with the power law except at 0.3 GPa. Swegle and Grady had also noted this sort of deviation when the shock stress is not much larger than the elastic limit.

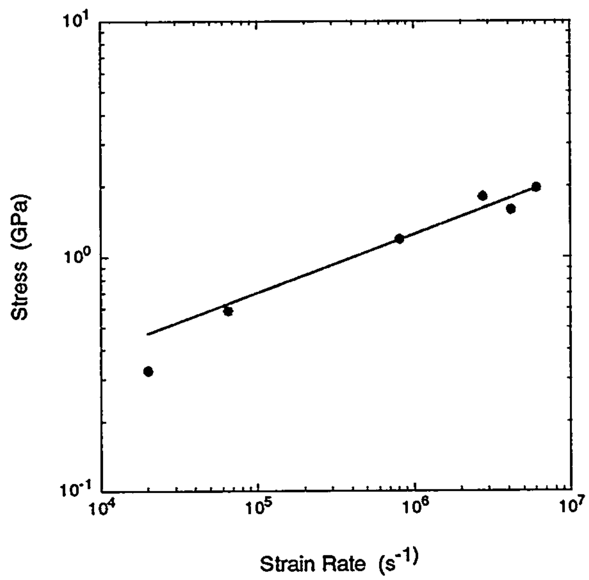

FIGURE 11. Comparison of the total strain rates of PBX 9501 for steady waves vs impact stress to the fourth power law.

ACKNOWLEDGMENTS

Jim N. Johnson provided helpful conversations, guidance, and sample calculations. Deanne Idar provided data and helpful comments. Some of the experiments were built by Dennis Price and Dave Kachelmeier.

REFERENCES

[1.] S. K. Chidester, C. M. Tarver, and C. G. Lee, Impact ignition of new and aged solid explosives, in *Shock Compression in Condensed Matter-1997*, edited by S. C. Schmidt, D. P. Dandekar, and J. W. Forbes, pages 707–710, Woodbury, NY, 1998, AIP.

[2.] B. W. Asay, G. W. Laabs, B. F. Henson, and D. J. Funk, J. Appl. Phys. **82**, 1093 (1997).

[3.] W. F. Hemsing, Rev. Scient. Instr. **50**, 73 (1979).

[4.] J. J. Dick, A. R. Martinez, and R. S. Hixson, Plane impact response of PBX 9501 and its components below 2 GPa, Technical Report LA-13426-MS, Los Alamos National Laboratory, Los Alamos, NM, 1998, Available in electronic form at www.lanl.gov.

[5.] T. R. Gibbs and A. Popolato, *LASL Explosive Property Data*, University of California Press, Berkeley, 1980.

[6.] B. Olinger and J. W. Hopson, Dynamic properties of some explosives and explosive simulants, in *Symposium H.D.P.*, pages 9–20, Saclay, 1978, Commissariat a l'Energie Atomique.

[7.] D. J. Idar, P. D. Peterson, P. D. Scott, , and D. J. Funk, Low strain rate compression measurements of PBXN-9, PBX 9501, and mock 9501, in *Shock Compression in Condensed Matter-1997*, edited by S. C. Schmidt, D. P. Dandekar, and J. W. Forbes, pages 587–590, Woodbury, NY, 1998, AIP.

[8.] J. Zaug, Elastic constants of β HMX as a function of pressure and temperature, in *Eleventhth Symposium (International) on Detonation*, 1998, to be published; also, private communication, 1997.

[9.] G. R. Fowles, J. Appl. Phys. **32**, 1475 (1961).

[10.] E. R. Lemar, J. W. Forbes, J. W. Watt, and W. L. Elban, J. Appl. Phys. **58**, 3404 (1961).

[11.] J. J. Dick, C. A. Forest, J. B. Ramsay, and W. L. Seitz, J. Appl. Phys. **63**, 4881 (1988).

[12.] L. C. Chhabildas and M. E. Kipp, Pressure-shear loading of PBX 9404, in *Eighth Symposium (International) on Detonation*, edited by J. M. Short, pages 274–283, White Oak, Maryland, 1986, Naval Surface Weapons Center NSWC MP 86-194, Naval Surface Weapons Center.

[13.] V. K. Mohan, V. C. J. Bhasu, and J. E. Field, Role of adiabatic shear bands in initiation of explosives by drop-weight impact, in *Ninth Symposium (International) on Detonation*, edited by W. J. Morat, pages 1276–1283, Arlington, Virginia, 1989, Office of Naval Research OCNR 113291-7, Office of Naval Research.

[14.] G. T. Gray, W. R. Blumenthal, C. M. Cady, and D. J. Idar, Influence of temperature on the high-strain-rate mechanical behavior of PBX 9501, in *Shock Compression in Condensed Matter-1997*, edited by S. C. Schmidt, D. P. Dandekar, and J. W. Forbes, pages 583–586, Woodbury, NY, 1998, AIP.

[15.] B. M. Dobratz and P. C. Crawford, LLNL Explosives Handbook, Technical Report UCRL 52997 Change 2, Lawrence Livermore National Laboratory, Livermore, CA, 1985.

[16.] D. Wiegand, Mechanical failure properties of composite plastic bonded explosives, in *Shock Compression in Condensed Matter-1997*, edited by S. C. Schmidt, D. P. Dandekar, and J. W. Forbes, pages 599–602, Woodbury, NY, 1998, AIP.

[17.] J. J. Dick and J. P. Ritchie, J. Appl. Phys. **76**, 2726 (1994).

[18.] J. W. Swegle and D. E. Grady, J. Appl. Phys. **58**, 692 (1985).